© 2015. Published by The Company of Biologists Ltd | Development (2015) 142, 3704-3712 doi:10.1242/dev.128736

RESEARCH ARTICLE

Facial whisker pattern is not sufficient to instruct a whisker-related topographic map in the mouse somatosensory brainstem

Christophe Laumonnerie[1,*,‡], Ahmad Bechara[1,‡], Nathalie Vilain[1], Yukiko Kurihara[2,3], Hiroki Kurihara[2,3] and Filippo M. Rijli[1,4,§]

ABSTRACT

Facial somatosensory input is relayed by trigeminal ganglion (TG) neurons and serially wired to brainstem, thalamus and cortex. Spatially ordered sets of target neurons generate central topographic maps reproducing the spatial arrangement of peripheral facial receptors. Facial pattern provides a necessary template for map formation, but may be insufficient to impose a brain somatotopic pattern. In mice, lower jaw sensory information is relayed by the trigeminal nerve mandibular branch, whose axons target the brainstem dorsal principal sensory trigeminal nucleus (dPrV). Input from mystacial whiskers is relayed by the maxillary branch and forms a topographic representation of rows and whiskers in the ventral PrV (vPrV). To investigate peripheral organisation in imposing a brain topographic pattern, we analysed *Edn1*$^{-/-}$ mice, which present ectopic whisker rows on the lower jaw. We found that these whiskers were innervated by mandibular TG neurons which initially targeted dPrV. Unlike maxillary TG neurons, the ectopic whisker-innervating mandibular neuron cell bodies and pre-target central axons did not segregate into a row-specific pattern nor target the dPrV with a topographic pattern. Following periphery-driven molecular repatterning to a maxillary-like identity, mandibular neurons partially redirected their central projections from dPrV to vPrV. Thus, while able to induce maxillary-like molecular features resulting in vPrV final targeting, a spatially ordered lower jaw ectopic whisker pattern is insufficient to impose row-specific pre-target organisation of the central mandibular tract or a whisker-related matching pattern of afferents in dPrV. These results provide novel insights into periphery-dependent versus periphery-independent mechanisms of trigeminal ganglion and brainstem patterning in matching whisker topography.

KEY WORDS: Whisker-related barrelette map, Mandibular brainstem representation, Topographic map, Hindbrain, Trigeminal ganglion, Trigeminal somatotopy, *Edn1*, *Cdh13*, *Tbx3*, *Hmx1*

INTRODUCTION

Relay of somatosensory stimuli from the body surface to higher brain centres is highly organised, allowing the sensing of positional origin of an input. Facial somatosensory inputs are serially relayed through the trigeminal circuit to the brainstem, thalamus and neocortex. The trigeminal circuit is somatotopically organised, such that topographic maps of connectivity matching the distribution and density of sensory receptors of facial dermatomes are generated at all levels of the pathway (Erzurumlu and Killackey, 1983; Erzurumlu et al., 2010; Ma, 1991, 1993; Ma and Woolsey, 1984; Schlaggar and O'Leary, 1993; Van Der Loos, 1976; Woolsey and Van der Loos, 1970).

Distinct facial dermatomes are innervated by the peripheral axonal processes of trigeminal ganglion (TG) primary sensory neurons, whose central axons form the trigeminal nerve (nV) and project to innervate second order neurons in the brainstem trigeminal column, composed of the rostral principal (PrV) and the caudal spinal (SpV) sensory nuclei. TG neurons bridge the facial sensory periphery and the brainstem where facial maps are first formed. During prenatal development, somatotopic segregation of TG cell bodies contributes to the segregation of the trigeminal nerve into its three main divisions – the mandibular, maxillary and ophtalmic branches, which peripherally innervate the corresponding facial dermatomes (Arvidsson and Rice, 1991; Erzurumlu and Jhaveri, 1992; Erzurumlu and Killackey, 1983; Erzurumlu et al., 2010; Hodge et al., 2007).

In mouse, the largest portion of the facial somatosensory map is devoted to the representation of mystacial whiskers which are organised into five rows of four to seven follicles at invariant positions on the snout. Whisker inputs are somatotopically mapped at each level of the pathway as spatially ordered neuronal modules, called barrelettes (brainstem), barreloids (thalamus), and barrels (cortex) (Ma and Woolsey, 1984; Van Der Loos, 1976; Woolsey and Van der Loos, 1970), reproducing facial whisker distribution.

The central axons of the mouse trigeminal nerve divisions start sending radially oriented collaterals at about embryonic day (E) 14.5 to innervate the PrV and SpV brainstem nuclei, and at about E16.5 begin to arborise, forming dense terminals (Erzurumlu et al., 2006; Ozdinler and Erzurumlu, 2002). In the developing PrV, mandibular axon collaterals selectively target the dorsal portion (dPrV) whereas whisker-related afferent collaterals preferentially target the ventral portion (vPrV) with a dorsoventral row-specific organisation (Erzurumlu and Killackey, 1983; Erzurumlu et al., 2010; Hodge et al., 2007; Oury et al., 2006; Xiang et al., 2010; this study). Thus, the spatial segregation of collateral targeting by distinct trigeminal divisions in PrV provides an early template to build topographic equivalence between the face and the brainstem.

To what extent peripheral signals and/or patterns are sufficient to impose a central somatotopic pattern is still debated. One approach to understanding a potential instructive role of the periphery in imposing a central somatotopic pattern has been to manipulate the number and/or spatial organisation of whiskers within the whisker pad. Such peripheral changes were reflected on the somatotopy of the barrel map (Ohsaki et al., 2002; Van der Loos et al., 1984). Moreover, retrograde signalling from the developing face was shown to be involved in establishing spatial patterns of gene

[1]Friedrich Miescher Institute for Biomedical Research, Maulbeerstrasse 66, Basel 4058, Switzerland. [2]Graduate School of Medicine, The University of Tokyo, 7-3-1 Hongo, Bunkyo-ku, Tokyo, 113-8654, Japan. [3]Core Research for Evolutional Science and Technology (CREST), Japan Science and Technology Agency (JST), Chiyoda-ku, Tokyo, 102-0075, Japan. [4]University of Basel, Basel 4056, Switzerland.
*Present address: St. Jude Children's Research Hospital, 262 Danny Thomas Place, Memphis, TN 38105, USA.
‡These authors contributed equally to this work

§Author for correspondence (filippo.rijli@fmi.ch)

Received 21 July 2015; Accepted 15 September 2015

Development (2015) 142, 3704-3712 doi:10.1242/dev.128736

expression in the TG and transferring somatotopic information to the brainstem (da Silva et al., 2011; Hodge et al., 2007). Such experiments seemed to indicate an instructive role of signalling from facial receptors to establish ordered connectivity at the peripheral and central level for somatotopic map generation.

By contrast, the early steps of cortical development and arealisation rely on intrinsic patterning mechanisms that are independent of sub-cortical input relaying information from the periphery (Cohen-Tannoudji et al., 1994; Grove and Fukuchi-Shimogori, 2003; López-Bendito and Molnár, 2003; O'Leary et al., 2007; Sur and Rubenstein, 2005). Furthermore, recent studies have begun to uncover some of the intrinsic molecular mechanisms underlying the establishment of somatotopic organisation at brainstem level (Erzurumlu et al., 2010; Oury et al., 2006). Thus, although facial pattern provides a template for map formation, it is still unclear whether it is sufficient to impose a central somatotopic pattern. Moreover, the relative importance of facial pattern to organise TG and central topography of connectivity at pre-natal stages, before facial maps are apparent at sub-cortical and cortical levels, is still poorly understood.

By using multicolour tracing methods, we first determined that a coarse row- and single whisker-specific somatotopic map is already built into somatosensory brainstem nuclei from the outset of the targeting process at pre-natal stages, with a relative degree of precision and peripheral positional discrimination. To investigate the importance of peripheral organisation in imposing a topographic pattern we took advantage of mutant mice exhibiting an ectopic whisker pattern on the lower jaw. In *Edn1* null mutant mice, the lower jaw is morphologically transformed into an upper jaw-like structure, including a partial duplication of the whisker pad with a second set of ordered whisker rows located in an ectopic, mandibular position (Fig. S1A) (Clouthier et al., 1998; Kurihara et al., 1994; Ozeki et al., 2004).

The $Edn1^{-/-}$ mutation is lethal at birth, thus preventing analysis at postnatal stages. Nonetheless, we found that, in $Edn1^{-/-}$ mutants, the ectopic whisker pad is innervated by mandibular, though not maxillary, TG neurons whose central axon collaterals initially targeted the dPrV. However, unlike maxillary neurons, ectopic whisker-innervating mandibular neurons and pre-target axons did not segregate into a row-specific pattern nor target the dPrV with a topographic pattern. Following periphery-driven molecular re-patterning to a maxillary-like identity, mandibular neurons redirected their central projections from dorsal to ventral PrV. Thus, a spatially ordered lower jaw ectopic whisker pattern is not sufficient to impose pre-target organisation of the mandibular tract nor a whisker-related matching pattern in dPrV, but it is still able to induce maxillary-like molecular features resulting in vPrV final targeting.

RESULTS

Whisker-related patterns of axon targeting are established prenatally in the hindbrain trigeminal nuclei

Distinct rows in the whisker pad are innervated by neuronal populations with segregated latero-medial distribution within the TG maxillary portion (da Silva et al., 2011; Erzurumlu and Jhaveri, 1992; Erzurumlu and Killackey, 1983; Hodge et al., 2007), whereas barrelette topography is not prefigured by a pre-ordered position of neurons within row-specific TG sub-populations (da Silva et al., 2011). We therefore investigated the establishment of whisker-specific afferent patterns in the developing brainstem and carried out row- and whisker-specific neuronal tracings with multicolour lipophylic NeuroVue fluorescent dyes, which allow controlled diffusion by progressive dye release from a filter membrane (Jensen-Smith et al., 2007).

By applying tiny pieces of NeuroVue-coated filters we simultaneously traced selected subsets of nerve endings innervating individual rows at E14.0. Single row-innervating primary neuron cell bodies segregated along the lateromedial axis of the maxillary TG portion (Fig. S2E). Furthermore, each set of single row-innervating nerve fascicles remained segregated in their central projections with a row-specific topography along the dorsoventral axis of the trigeminal tract maxillary division (Fig. S2A-E). These results confirmed a high degree of order in the trigeminal peripheral system during prenatal development (Erzurumlu and Killackey, 1983) and supported the validity of our tracing procedure.

To investigate the spatial arrangement of whisker-specific central collateral targeting, we simultaneously labelled distinct anteroposterior whisker follicle positions in different rows of E14.5 and E17.5 whisker pads (Fig. S2F-I). The insertion of NeuroVue filters at single follicles allowed targeting of the follicle terminals and just their close neighbours. To improve tracing precision, we selectively labelled whiskers at distinct positions where they are bigger and less densely spaced (position 1-5) (Fig. S2J). Along the dorsoventral axes of the vPrV and SpVi nuclei, collaterals maintained the row-specific somatotopy observed in the trigeminal tract (Fig. S2F,H and not shown) (Xiang et al., 2010). Notably, collaterals from afferents innervating anterior whiskers projected deeper medially into the vPrV nucleus than collaterals of posterior whisker positions (colour bars, Fig. S2F,H). The early somatotopic pattern of whisker-specific collateral targeting was maintained and further refined by E17.5 (Fig. S2G,I). At this stage, collaterals showed dense arborisation, prefiguring maturation of the final whisker map and barrelette formation as observed by cytochrome oxidase staining at postnatal (P) stages (P6, Fig. S2K).

In summary, these results further extend previous work. They show that the topographic mapping of row-specific and single whisker-specific afferent targeting in brainstem nuclei is established at the onset of collateralisation with a relative degree of precision and peripheral positional discrimination, and is refined throughout late prenatal and early postnatal stages.

Ectopic whisker arrays in $Edn1^{-/-}$ mutants are innervated by trigeminal mandibular primary neurons

We first asked whether the ectopic whisker pad of *Edn1* null mutants is innervated and by which TG division. We carried out triple retrograde labelling at E14.5 and applied NeuroVue at the ectopic whisker pad on the mutant lower jaw and at two dorsoventral positions in the maxillary whisker pad (Fig. 1C,D). The neurons innervating the ectopic whiskers, traced in a retrograde manner, were located in the mandibular portion of TG and were segregated from those in the maxillary division wiring the normal whisker pad (Fig. 1E,F). Thus, the ectopic whisker pad on the lower jaw of $Edn1^{-/-}$ mutants is not able to attract and redirect the peripheral projections of maxillary primary sensory neurons.

Furthermore, the central axon of neurons innervating the duplicated whisker pad did not intermingle with the axons of the neurons innervating the maxillary whisker pad and maintained the same dorsally segregated position in the trigeminal tract of $Edn1^{-/-}$ fetuses as that of mandibular axons in wild type (Fig. 1G,H).

Induction of maxillary-like molecular features in $Edn1^{-/-}$ mutant mandibular primary neurons upon ectopic whisker pad innervation

Bmp4 and TGF-β retrograde signalling from the whisker pad and/or follicles has been suggested to be involved in organising

Development (2015) 142, 3704-3712 doi:10.1242/dev.128736

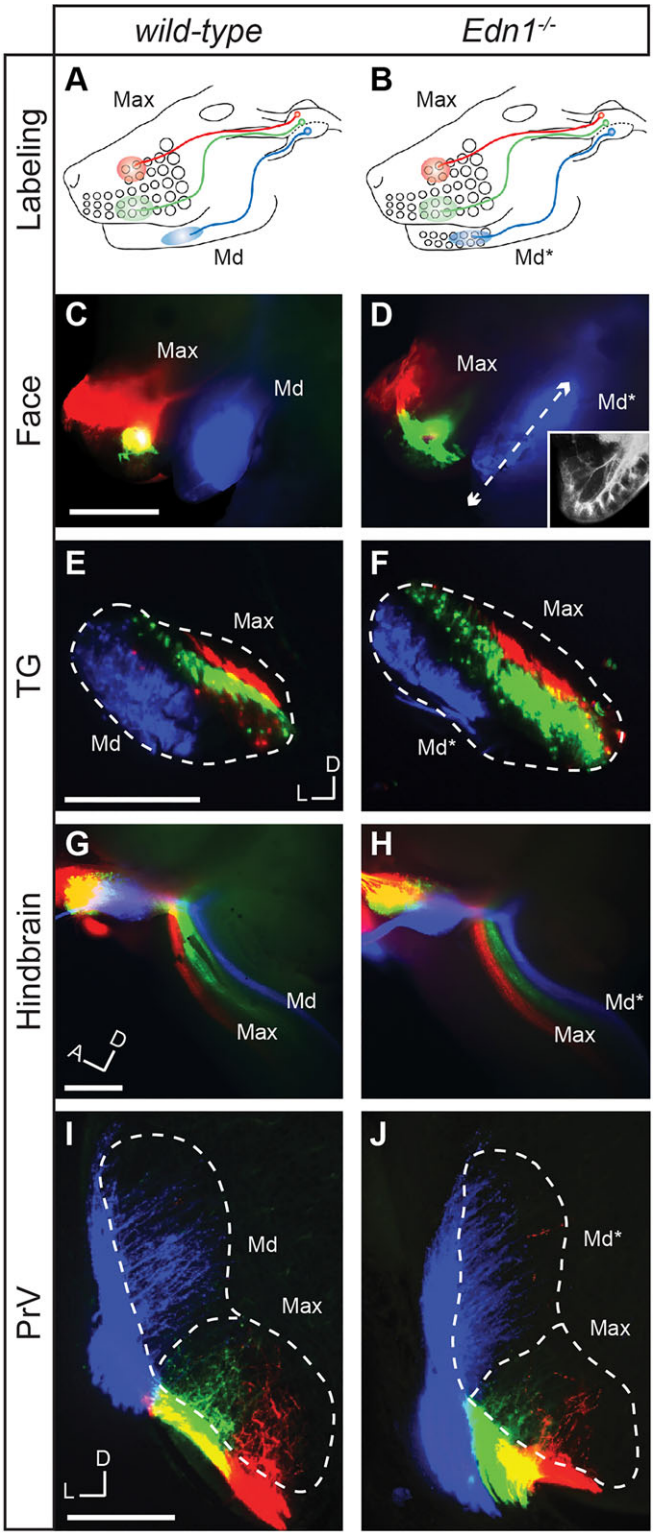

Fig. 1. Ectopic whisker pad innervation in *Edn1* null mutant fetuses. E14.5 wild-type (A,C,E,G,I) and *Edn1*$^{-/-}$ (B,D,F,H,J) fetuses showing labelling of mandibular (Md) (blue), lower (green), or upper (red) maxillary (Max) whisker row positions. (C,D, inset) wild-type Md and *Edn1*$^{-/-}$ ectopic whisker pad (Md*) innervation, summarised in A,B. Arrow represents the section plan for the inset showing ectopic follicle innervation. (E,F) Trigeminal ganglion (TG) coronal section showing retrograde tracing of mandibular neurons innervating wild-type mandible (Md) (E) and ectopic *Edn1*$^{-/-}$ whisker pad (Md*) (F). (G) Lateral view showing wild-type dorsoventral segregation of central trigeminal axon bundles relaying distinct Max and Md positions. (H) Ectopic whisker pad (Md*) innervation in *Edn1*$^{-/-}$ fetuses does not change pre-target central axon ordering within the tract. (I,J) Principal nucleus (PrV) coronal sections showing similar dorsoventral distribution of central afferent collaterals in wild-type (I) and *Edn1*$^{-/-}$ (J) fetuses. Note segregation of mandibular (blue) and maxillary (green and red) inputs in dorsal and ventral PrV, respectively. Scale bars: 200 µm in C,D; 100 µm in E-H; 50 µm in I,J.

topographic patterns of TG neuron central connectivity (da Silva et al., 2011; Hodge et al., 2007). In particular, Bmp4-dependent signalling regulates early positional differences of Tbx3 and Hmx1 transcription factor expression in distinct divisions of the TG (Hodge et al., 2007). *Bmp4* expression is readily detected in the duplicate arrays of whisker primordia on the *Edn1*$^{-/-}$ mutant lower jaw (Ozeki et al., 2004). We therefore asked whether maxillary-like spatial patterns of transcription factor expression were ectopically induced in the mandibular division of *Edn1*$^{-/-}$ mutants upon innervation of the duplicated whisker pad.

In wild-type E11.5 and E13.5 TG, *Hmx1* and *OC1* (*Onecut1* – Mouse Genome Informatics) are selectively expressed in the mandibular division, whereas *Tbx3* is highly expressed in ophthalmic and maxillary neurons with only sparse expression in mandibular neurons (Fig. 2B-D) (Hodge et al., 2007). In *Edn1*$^{-/-}$ mutants, expression of the general marker *Drg11* (*Prrxl1* – Mouse Genome Informatics) was normally maintained throughout the TG (Fig. 2A,E,L,N). By contrast, *Tbx3* was induced in a larger number of mandibular neurons than in wild type, whereas *Hmx1*$^{+}$ and *OC1*$^{+}$ cells were concomitantly reduced (Fig. 2F-H). This was further confirmed with *Hmx1*/*Tbx3* double fluorescent *in situ* hybridisation (FISH) and quantified (Fig. 2I-K). This effect was not a result of increased cell death in the mandibular TG component, as assessed by activated caspase-3 immunostaining (Fig. S3A,B). Moreover, no *Tbx3* expression differences were observed at E10.25 between wild-type and *Edn1*$^{-/-}$ TG neurons (Fig. S3G,L), indicating that the molecular changes observed in E11.5 *Edn1*$^{-/-}$ mandibular neurons are induced as their axons grow into the duplicated whisker pad.

To further support a periphery-induced re-patterning of mandibular neurons in *Edn1*$^{-/-}$ mutants, we next searched for additional TG maxillary-specific expression markers in the Allen Developing Mouse Brain Atlas (http://developingmouse.brain-map.org). At E13.5, cadherin 13 (*Cdh13*) is selectively expressed in the maxillary TG division, whereas it is excluded from the mandibular division (Fig. 2M). By combining retrograde dextran tracing of row-specific afferents and *Cdh13* in situ hybridisation at E13.5, we further assessed that *Cdh13* is preferentially expressed in TG neurons innervating row C-E (Fig. S3C-F). As these rows are duplicated in a mirror pattern in *Edn1*$^{-/-}$ mutants (Ozeki et al., 2004) (Fig. S1), we assessed *Cdh13* expression in E13.5 mutant TG. Notably, *Cdh13* was ectopically induced in the mandibular division of *Edn1*$^{-/-}$ mutants (Fig. 2O).

In summary, these findings demonstrate that positional molecular differences are induced in *Edn1*$^{-/-}$ mutant TG, leading a subset of mandibular neurons to acquire molecular features normally expressed by maxillary primary sensory neurons innervating mystacial whiskers.

The ectopic whisker pad is not sufficient to impose maxillary-like topography to mandibular central axons in *Edn1*$^{-/-}$ mutants

We next asked whether the observed molecular changes were sufficient to induce corresponding maxillary-like changes in the central topography of TG mandibular neurons in *Edn1*$^{-/-}$ fetuses.

Development (2015) 142, 3704-3712 doi:10.1242/dev.128736

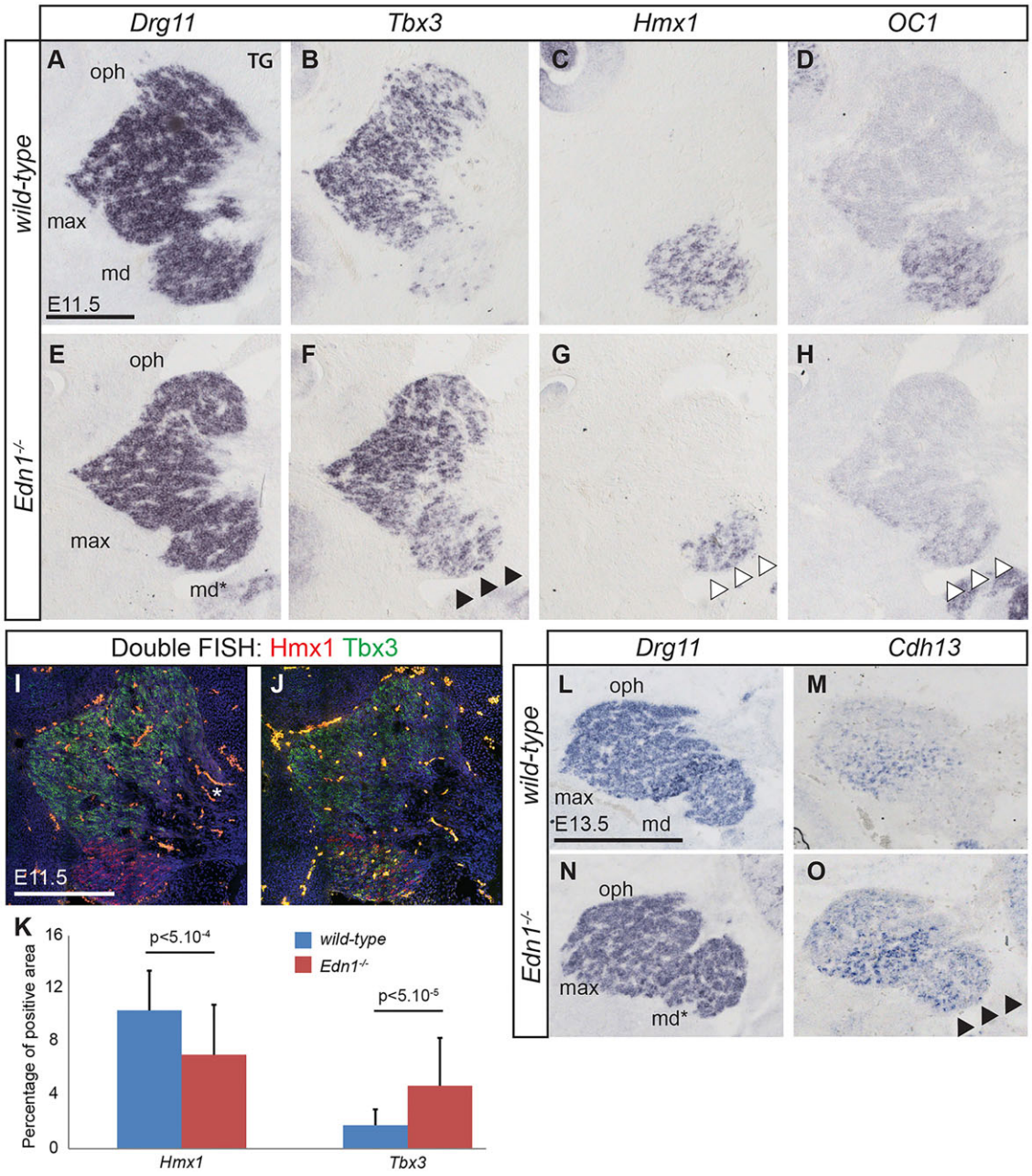

Fig. 2. Induction of maxillary-like molecular features in *Edn1* mutant mandibular primary neurons. (A-H,L-O) Sagittal sections through trigeminal ganglion (TG) mandibular (md), maxillary (max), and ophthalmic (oph) divisions at E11.5 and E13.5 in wild-type (A-D,L,M) and *Edn1*$^{-/-}$ (E-H,N,O) littermates hybridised with *Drg11* (A,E,L,N), *Tbx3* (B,F), *Hmx1* (C,G), *OC1* (D,H), and *Cdh13* (M,O) probes. In *Edn1*$^{-/-}$ mutant md (md*) (F-H,O), *Tbx3* expression is increased (F, black arrowheads), *Hmx1* and *OC1* (G,H, white arrowheads) decreased, and *Cdh13* ectopically induced (O, black arrowheads). (I-K) *Hmx1* and *Tbx3* double fluorescent *in situ* hybridisation and quantification of positive area showing significant *Hmx1* signal reduction and *Tbx3* increase in wild-type (I) and *Edn1*$^{-/-}$ (J) littermates at E11.5. Note that the yellow/orange bright spots correspond to aspecific background as a result of blood vessel autofluorescence (e.g. asterisk in I). (K) Quantification of *Hmx1* and *Tbx3* expression. The graphs represent the mean±standard deviation percent of positive pixels above threshold within the mandibular area (wild type, *n*=33 sections; *Edn1*$^{-/-}$, *n*=29 sections; from five embryos each). Scale bars: 50 µm in A-J; 100 µm in L-O.

We assessed whether the tract innervating the duplicated arrays of whiskers in *Edn1*$^{-/-}$ mutants also became somatotopically organised, in the same manner as maxillary tract organisation (Fig. S1). In wild-type fetuses (*n*=4/stage), NeuroVue labelling of two distinct positions at E14.5 and E16.5 on the lower jaw (Fig. 3A, Fig. S4A) revealed intermingled non-segregated primary neuron cell bodies in the mandibular TG division (Fig. 3C, Fig. S4B). This was further depicted in the lack of spatial segregation of mandibular afferent central axons (Fig. 3E, Fig. S4C-D), contrasting with the strict somatotopic organisation of the maxillary tract (*n*=4/stage) (Fig. 1C, Fig. S2E).

Similarly, in E14.5 and E16.5 *Edn1*$^{-/-}$ mutant fetuses (*n*=4/stage), despite the ectopic whisker arrays on the lower jaw, NeuroVue labelling of two distinct ectopic row positions (Fig. 3B, Fig. S4E) also resulted in a non-segregated distribution of retrogradely labelled cell bodies in the TG (Fig. 3D, Fig. S4F) and a lack of somatotopic organisation of central axons (Fig. 3F, Fig. S4G,H), similar to wild-type mandibular branch organisation.

Development (2015) 142, 3704-3712 doi:10.1242/dev.128736

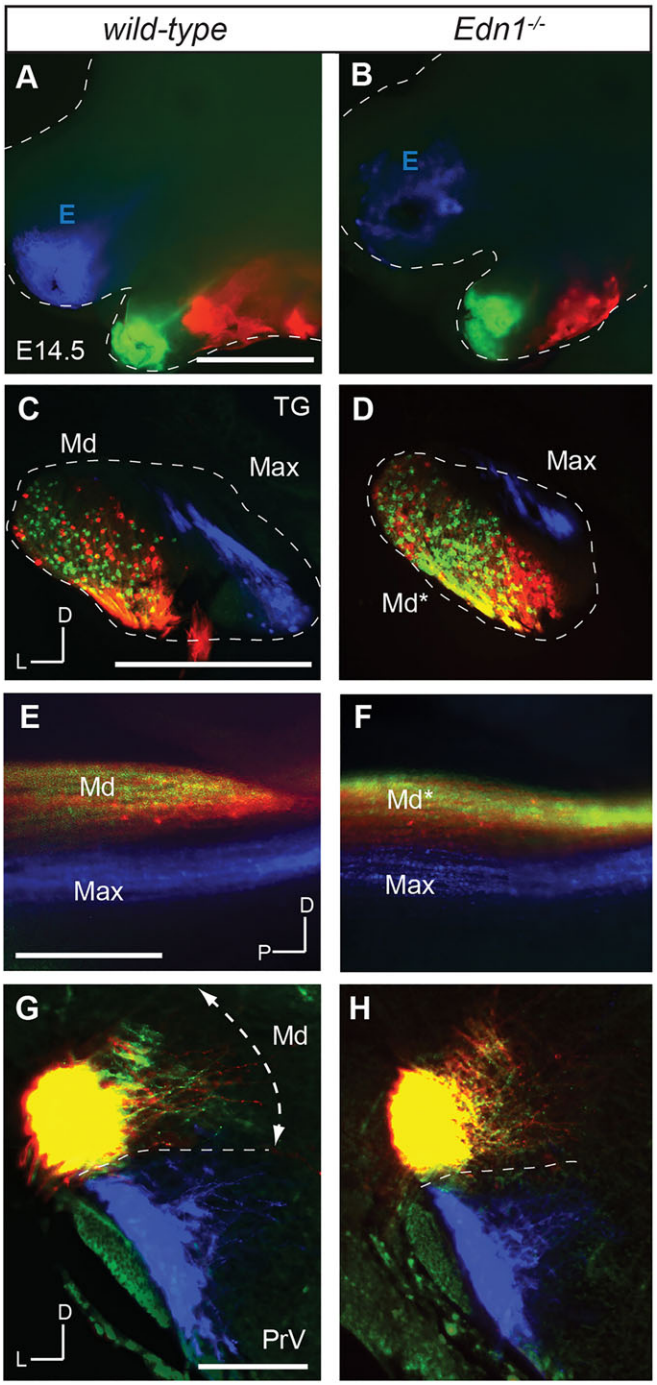

Fig. 3. Poor topographic organisation of mandibular trigeminal nerve branch and central axon projections in wild-type and *Edn1*$^{-/-}$ fetuses. Labelling of distinct positions of mandibular process in E14.5 wild-type (A,C,E, G) and *Edn1*$^{-/-}$ (B,D,F,H) fetuses. (A,B) Lateral face view with row E (blue), anterior-dorsal (green) and posterior-ventral (red) mandibular position labelling in wild type (A) and *Edn1*$^{-/-}$ (B). (C-F) Trigeminal ganglion (TG) coronal sections (C,D) and whole-mount trigeminal tract lateral views (E,F). In wild-type (C,E) and *Edn1*$^{-/-}$ (D,F) fetuses, neurons innervating distinct lower jaw positions show no clear spatial segregation of cell bodies in TG mandibular division (Md and Md*, respectively) nor of their central axons within the mandibular tract. Max, maxillary neurons (C,D) and tract (E,F). (G,H) Principal nucleus (PrV) coronal sections of wild-type (G) and *Edn1*$^{-/-}$ (H) fetuses showing lack of targeting collateral topographic organisation of sensory neurons innervating the two distinct positions labelled on the mandibular process in A and B. Arrow indicates the area of mandibular collateral spreading. Scale bars: 200 µm in A,B; 100 µm in C-F; 50 µm in G,H.

Thus, the maxillary-like molecular changes induced in neurons innervating the duplicated whisker rows in *Edn1*$^{-/-}$ mutants (Fig. 2) are not sufficient to impose a maxillary-like topography to their central afferents.

Ectopic whisker-innervating afferents initially project in dPrV without generating ordered collateral patterns but redirect their projection to vPrV at late prenatal stages

We then investigated the central pattern of collateral targeting in E14.5 *Edn1*$^{-/-}$ mutants. In wild-type fetuses, mandibular TG axons project radially oriented collaterals into rhombomere (r)2-derived dPrV, whereas r3-derived vPrV selectively receives collateral input from whisker-related afferents (Oury et al., 2006). These distinct populations of targeting collaterals remain spatially segregated within the PrV and never cross each other (Fig. 1H, Fig. 3G, Fig. 4C,D,I,J) (Oury et al., 2006). In *Edn1*$^{-/-}$ mutants, axon afferents from the duplicated whisker arrays did not project collaterals into the vPrV area which normally hosts the whisker map but instead targeted the dPrV area which normally generates the lower jaw map (Fig. 1J). Moreover, labelling of distinct peripheral positions on the lower jaw did not result in spatially segregated collaterals along either the row-specific dorsoventral or whisker-specific lateromedial axes in the dPrV (Fig. 3H), in contrast to the whisker-related collateral topographic mapping observed in the vPrV (Fig. 1I, Fig. S2F-I).

Remarkably, unlike at E14.5, at E16.5 ectopic whisker (Md*)-innervating collaterals turned from dPrV (and dorsal SpV), and navigated into vPrV (and ventral SpV) (arrows, Fig. 4G,H, Fig. S4G,H). Upon labelling of two distinct ectopic row positions no clear sorting of collaterals navigating into vPrV or ventral SpV was observed (arrows, Fig. S4G-H). The fraction of collaterals attracted ventrally was variable (roughly 5-40%) (see Fig. 4G-H, Fig. S4G-H). This variability likely depended on the precision and/or amount of labelling of the ectopic whisker follicles versus the surrounding lower jaw tissue in each experiment and/or on the extent of mandibular neuron repatterning among distinct *Edn1*$^{-/-}$ mutant individuals. Nonetheless, such a mis-targeting behaviour of Md* collaterals was observed in all mutants (n=6/6) and never in wild type (n=6/6) (quantified in Fig. 4I,J).

Thus, the Md* primary neurons innervating the duplicated whisker pad in *Edn1*$^{-/-}$ mutants initially project central axon collaterals into dPrV, similar to normal lower jaw input. Despite the observed maxillary-like molecular changes as early as E11.5 (Fig. 2), these Md* incoming afferents are unable to generate ordered ectopic whisker-related patterns of collateral targeting in dPrV, unlike the maxillary whisker afferents in vPrV. However, the molecular changes in Md* TG neurons might enable ectopic whisker afferents to respond to late vPrV-specific targeting cues prior to barrelette formation (Fig. 4K,L).

DISCUSSION

Brainstem whisker maps develop through interplay between peripheral signals, intrinsic pre-patterning of TG neurons with their axonal processes, and brainstem target neurons, establishing a prenatal coarse topographic connectivity map. Further refinement by whisker-related activity and/or retrograde molecular signalling from periphery contributes to achieve final one-to-one topography at postnatal stages. Recent studies addressed the importance of facial signals to refine central projections (da Silva et al., 2011; Hodge et al., 2007) whereas others highlighted the importance of brainstem patterning to receive appropriate and spatially restricted peripheral projections and allow topographic representation (Erzurumlu et al.,

Development (2015) 142, 3704-3712 doi:10.1242/dev.128736

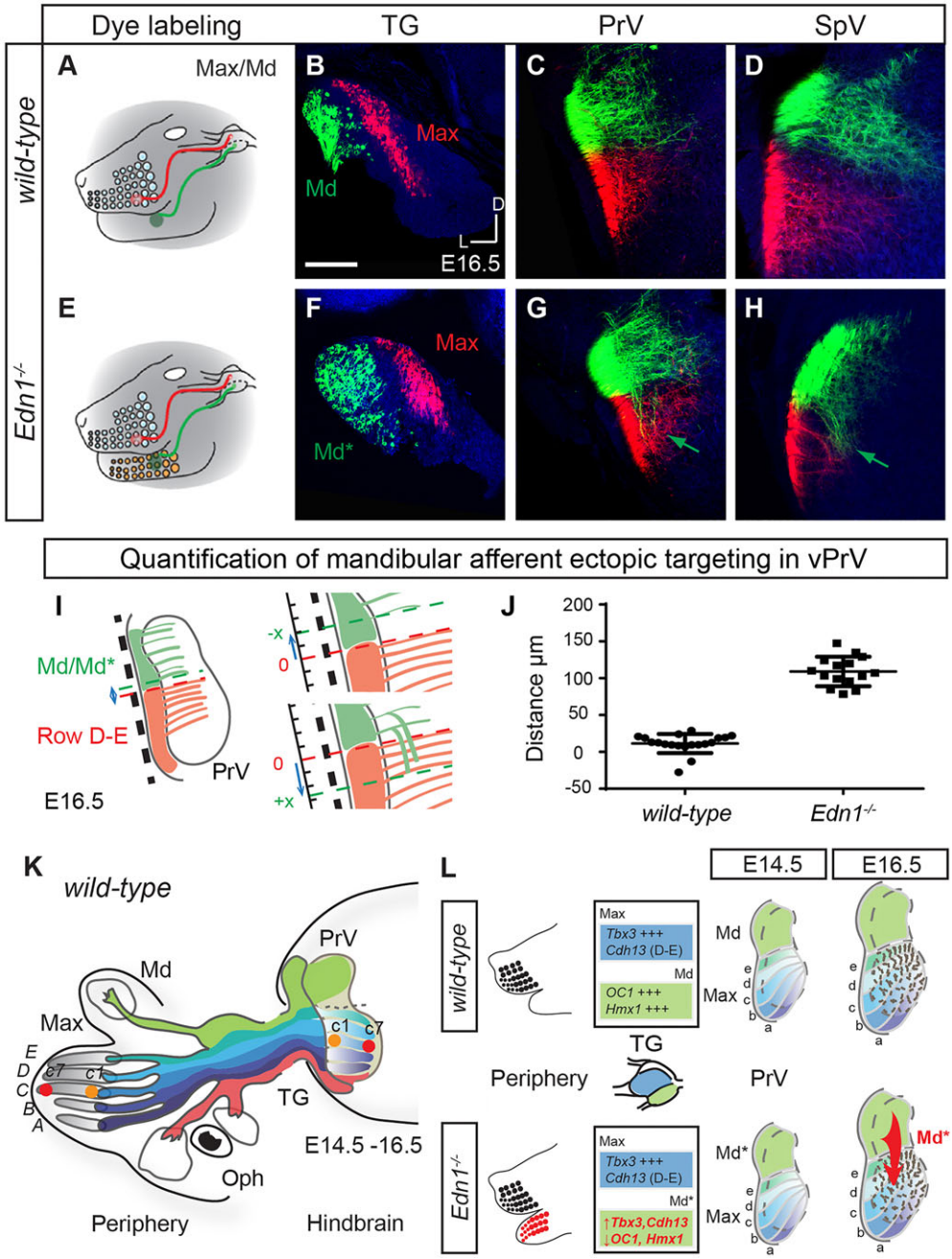

Fig. 4. Late redirection of mandibular central axon projections from dorsal to ventral PrV and SpV in *Edn1*$^{-/-}$ fetuses. (A-H) Distinct position labelling of maxillary (Max) and mandibular (Md) facial processes in E16.5 wild-type (B-D) and *Edn1*$^{-/-}$ (F-H) fetuses. (A,E) Diagram of dye labelling of lower maxillary (red) and mandibular (green) positions corresponding to sections (B-D,F-H). Trigeminal ganglion (TG) (B,F), principal nucleus (PrV) (C,G) and spinal nucleus (SpV) (D,H) coronal sections. In *Edn1*$^{-/-}$ (G,H), ectopic whisker-innervating mandibular (Md*) axon collaterals targeting dPrV and dorsal SpV turn ventrally into vPrV and ventral SpV (arrows). (I) Method for phenotype quantification. An axis was set parallel to the lateral border of the PrV (black dashed line). The dorsal-most position of maxillary collaterals (red dashed line) was set as 0. The ventral-most position reached by mandibular collaterals (green dashed line) was measured on the axis, and counted as negative for a gap or as positive if invading the maxillary collateral domain (considering the furthest axon invading the inappropriate area). (J) Quantification of mandibular-maxillary collateral overlap, distance (in µm) of furthest axon from position 0 as defined in I (wild type, *n*=19 sections; *Edn1*$^{-/-}$, *n*=15 sections; from five embryos each). (K) Diagram of trigeminal pathway somatotopy at E14.5-E16.5. The trigeminal nerve is dorsoventrally sorted in ophthalmic (Oph), maxillary (Max) and mandibular (Md) branches. In trigeminal ganglion (TG), Max neuron cell bodies additionally display whisker row-specific lateromedial spatial segregation. Row- and whisker position-specific information is coarsely topographically mapped by Max neuron collaterals emerging from the central sensory tract along dorsoventral and mediolateral axes of ventral PrV, respectively, as early as E14.5 and progressively refined. By contrast, TG Md neurons innervating distinct mandible positions, their central axons, and dorsal PrV collateral targeting display poor somatotopic segregation. C1 (orange dot) and C7 (red dot) whiskers illustrate whisker-specific distribution of afferent collaterals targeting the lateromedial axis of PrV. (L) Schematic depicting *Edn1*$^{-/-}$ phenotype and molecular changes. In *Edn1*$^{-/-}$ fetuses, spatially ordered ectopic whiskers are not sufficient to induce row-specific axon sorting in the TG mandibular branch nor of its central projections that initially target dorsal PrV. Nevertheless, upon innervation of ectopic whiskers, Md neurons acquire molecular features of Max neurons (Md*) that, at later stages, lead Md* collaterals to navigate out of the 'lower jaw map' area in dorsal PrV and enter the 'whisker map' area in ventral PrV. Gene expression in the Max (blue) or Md (green) TG subdivisions of wild-type fetuses and gene expression increase or decrease (arrows) in Md* of *Edn1*$^{-/-}$ mutants; labels a-e represent row-specific afferents; red arrow indicates Md* collaterals redirected towards vPrV. Scale bars: 50 µm in B-D,F-H.

Development (2015) 142, 3704-3712 doi:10.1242/dev.128736

2010; Oury et al., 2006). However, the relative importance of facial signals versus TG pre-target axon sorting versus central pre-patterning in the building of topographic equivalence between the face and the brainstem is still unclear. In this study, we asked whether an ordered array of whisker receptors on the face is sufficient to impose a matching topographic connectivity into the brainstem, in order to unveil the relative contributions of specific TG neuron pre-sorting events and/or central pre-patterning.

A number of conclusions can be drawn from our study. Firstly, we provide evidence that, in addition to a row-specific somatotopy of maxillary pre-targeting axons, a single-whisker map of afferent collateral targeting is set out in vPrV from the outset of the collateralisation process with a significant degree of precision and peripheral positional discrimination, which is progressively refined through late prenatal and postnatal stages (Fig. S2). Thus, postnatal activity-dependent refinement processes might only act locally to stabilise pre- and post-synaptic elements, but they are not the main contributors to building an ordered whisker-specific topography within the brainstem sensory nuclei. This is supported by the analysis of NMDA receptor knockout mice, in which barrelette neuron dendrite remodelling and patterning is impaired, but the general topographic organisation of afferents is maintained in mutant PrV (Lee et al., 2005).

Secondly, we show that the central axons of TG mandibular neurons innervating distinct lower jaw surface positions display poor spatial segregation within the mandibular tract, as do their collateral patterns in dorsal PrV. Our analysis of *Edn1*$^{-/-}$ mutants further demonstrate that ectopic whisker arrays are selectively targeted by the mandibular branch, according to their position on the lower jaw, and that this innervation in turn induces significant maxillary-like molecular changes in mandibular TG neurons, supporting whisker-specific retrograde signalling (da Silva et al., 2011; Hodge et al., 2007). However, such molecular changes are not sufficient to instruct a maxillary-like, row-specific, pre-target axon sorting of the mandibular tract, nor to instruct the establishment of row- and/or whisker-related patterns of collateral targeting in the dorsal 'mandibular' area of PrV. Together, these findings highlight a fundamental intrinsic pre-ordering difference between TG maxillary and mandibular primary axons which will be important to address in future studies. Pre-ordering of somatosensory thalamocortical axons is essential for the transfer of precise topographic equivalence between thalamic and cortical whisker maps (Lokmane et al., 2013). Our current results suggest that maxillary neuron pre-target axon pre-ordering (Erzurumlu and Jhaveri, 1992; Erzurumlu and Killackey, 1983; reviewed in Erzurumlu et al., 2010) might be intrinsically organised, independently of facial or brainstem influences, and might be an important spatial requisite to match intrinsic positional information in the vPrV (see summary diagram in Fig. 4K,L).

Lastly, even though ectopic whisker-innervating mandibular axons initially target the dPrV, following periphery-driven repatterning their collaterals turn and navigate from dorsal to ventral PrV, converging into the whisker-related area already occupied by the processes of maxillary neurons innervating the normal whisker pad on the snout (Fig. 4). These latter findings unveil a temporal sequence of events underlying the transfer of peripherally induced whisker-specific information to the brainstem and suggest the importance of a vPrV-specific intrinsic patterning program to match whisker-specific input. Further studies will be required to address the molecular determinants of such a program. In this respect, it is however noteworthy that *Hoxa2* displays a differential expression pattern between dPrV and vPrV, and has an important role in prenatal PrV patterning (Oury et al., 2006). *Hoxa2* is expressed in all PrV mitotic progenitors but differentially maintained in the post-mitotic neurons of vPrV, though not dPrV (Oury et al., 2006). Moreover, *Hoxa2* is not expressed in TG neurons or facial mesenchyme (Oury et al., 2006). The early dorsoventral differential expression of *Hoxa2* regulates the specific targeting of mandibular versus maxillary trigeminal axon collaterals between the dorsal and ventral components of the developing PrV (Erzurumlu et al., 2010; Oury et al., 2006). In particular, conditional *Hoxa2* inactivation selectively impaired whisker-related afferent targeting in the vPrV (Oury et al., 2006), indicating that *Hoxa2* might regulate the expression of whisker afferent collateralisation factor(s) in vPrV. Brainstem maturation is a crucial regulator of the onset of arborisation of trigeminal ganglion afferents in brainstem nuclei (Erzurumlu et al., 2010; Ozdinler and Erzurumlu, 2002). Prenatal row- and whisker-specific afferent topographic collateralisation could be under the control of collateral-target interactions mediated by differentially expressed surface-bound and/or secreted guidance molecules (Erzurumlu et al., 2010). In this regard, *Hoxa2* has been shown to positively regulate *Epha4* and *Epha7* expression in vPrV (Oury et al., 2006). Moreover, our finding that *Cdh13* displays row-related expression in TG neurons suggests that matching adhesive cues between central afferent axons and brainstem target neurons might also contribute to topographic collateralisation into vPrV. Lastly, dPrV is devoid of *Hoxa2* expression at the stage of collateral formation (Oury et al., 2006). Thus, the lack of topographic patterns of collateral targeting observed in *Edn1* mutant dPrV, which receives selective input from the duplicated whisker arrays (Fig. 4), might at least partly account for the lack of a *Hoxa2*-dependent patterning program that normally instructs prenatal afferent targeting topography and establishment of whisker-related patterns in vPrV.

MATERIALS AND METHODS

Mouse strains

Edn1^{tm1Utj} (referred to as *Edn1*$^{-/-}$) homozygous mutant mice were described (Kurihara et al., 1994). Each *in situ* hybridisation and tracing experiment at any given stage was carried out on at least n=3 *Edn1*$^{-/-}$ mutant and control embryos and fetuses; some tracing experiments were carried out on n=4 or n=6 mutant and control fetuses, respectively, as indicated in the main text. All animal experiments were approved by local veterinary authorities and conducted in accordance with the Guide for Care and Use of Laboratory Animals.

Simple and double *in situ* hybridisation

Embryos were dissected and fixed in 4% paraformaldehyde/PBS (PBS–PFA4%) overnight at 4°C. Tissues were cryoprotected in 20% sucrose and embedded in gelatine with 7.5%/10% sucrose/PBS. Cryostat sections (20-25 µm) in coronal and sagittal orientations were frozen at −80°C until processing. For chromogenic *in situ* hybridisation, the *OC1*, *Tbx3* and *Hmx1* (Hodge et al., 2007) probes were a gift from F. Wang. The *Cdh13* probe was generated by cloning nucleotides 1139-2145 from the coding sequence into a pCRII-TOPO vector using a TOPO TA cloning kit (Life Technologies). Fluorescent *in situ* hybridisations were performed using the RNAscope Multiplex Fluorescent Kit according to the manufacturer's protocol [Advanced Cell Diagnostics (ACD), ref: 320850]. In brief, sections were air dried for 30 min at room temperature (RT), and a hydrophobic barrier was drawn around sections with an Immedge hydrophobic barrier pen. Sections were incubated for 20 min with the protease solution Pretreat 4 (RNAscope Pretreatment Kit) at RT in a humid chamber, washed twice with PBS and then incubated with the mixture of *Tbx3* and *Hmx1* probes for 2 h at 40°C in an oven. cDNA probe sets were designed and generated by ACD. Targeted sequences were: Mm-*Tbx3*-C1, nucleotides 460-1597 of accession number NM_011535.3 and Mm-*Hmx1*-C2, nucleotide 109-1483 of

Development (2015) 142, 3704-3712 doi:10.1242/dev.128736

accession number NM_010445.2. A probe against the gene encoding POL2RA, a protein expressed in mammalian cells, was used as positive control, and a probe against *Escherichia coli dapB* (not expressed in mammalian cells) was used as a negative control (data not shown). Sections were then incubated with preamplifier and amplifier probes by applying AMP1 (40°C for 30 min), AMP2 (40°C for 15 min), and AMP3 (40°C for 30 min), followed by incubation with AMP4 AltA (40°C, 15 min), containing fluorescently labelled probes to detect *Tbx3* RNA in green (Alexa Fluor 488, ACD), and *Hmx1* RNA in orange (Alexa Fluor 550, ACD). A final incubation of slides with DAPI (ACD) for 30 s was performed before mounting them with Prolong Gold antifade reagent (Molecular Probes, P36934). Imaging of fluorescent signals was performed using an Axio Imager Z2 upright microscope coupled to a LSM700 Zeiss laser scanning confocal at 40×. Maximum intensity projections and stitching of double fluorescent *in situ*s were performed using ZEN Software (Zeiss).

Immunohistochemistry

Cryosections were immunolabelled with a rabbit primary antibody against active Caspase-3 (1:500; Promega, G748A), and goat anti-rabbit Alexa Fluor 568-conjugated antibody (1:200; Molecular Probes, A-11011), counterstained with DAPI and mounted with Prolong Gold antifade reagent.

Cytochrome oxidase staining

For cytochrome oxidase (CO) histochemical staining (Fig. S2K), 40 µm cryostat sections were cut in the coronal plane to visualise barrelettes at brainstem levels. The CO staining was performed according to the procedure described in Wong-Riley (1979).

NeuroVue dye-coated filters labelling

NV Red (FS-1002), NV Maroon (FS-1001) and NV Jade (FS-1006) NeuroVue dye-coated filters were from Molecular Targeting Technologies (West Chester, PA, USA). Embryos were fixed in PBS–PFA4% overnight at 4°C. Small pieces (<1 mm²) of NeuroVue filter dyes were cut and placed into the specimen at specific locations. Embryos and fetuses were incubated at 37°C for 2 weeks (E10.5, E11.5), 3 weeks (E12.5), 4 weeks (E14.0, E14.5) or 6 weeks (E16.5, E17.5) in PBS–PFA4%. Diffusion of staining around the injection sites was monitored using a MacroFluo Z6 APO (Leica Microsystems). Whole-mount brains were dissected, keeping trigeminal ganglion attached to the brain, and imaged. Flat-mount preparations of E10.5 and E11.5 embryos were obtained by dissecting the neural tube, mounting in PBS between a slide and a cover slip and imaging. Older embryos were embedded into 4% agarose. Vibratome sections of 50-100 µm were mounted in Aqua-Poly/Mount (Polysciences) and analysed under MacroFluo Z16 APO and confocal microscope (LSM700, Zeiss).

Retrograde labelling of single whisker with dextran

Biotin-conjugated lysine-fixable dextran (Invitrogen, D-7135) was employed for retrograde labelling of specific whisker rows in E13.5 mouse fetuses. Dextran crystals were prepared according to Stirling et al. (1995). E13.5 fetuses were dissected and labelled with dextran crystals in given whisker follicle, cultured for 6 h as described previously (Oury et al., 2006; Stirling et al., 1995), then fixed in PBS–PFA4% and prepared for cryosection as described above. Sagittal sections of 25 µm were collected and processed for chromogenic *in situ* hybridisation against *Cdh13*. Biotin was revealed afterward using fluorescent-conjugated streptavidin (1:200; Molecular Probes, S11223), mounted and analysed under fluorescence microscope (Olympus).

Image analysis

Brightness, contrast and gamma (not for *in situ* hybridisation) were adjusted in Adobe Photoshop 2015 for better visualisation, and figures assembled in Adobe Illustrator 2015. Quantification of double fluorescent *in situ* in Fig. 2 was realised using Slidebook 6 (Intelligent Imaging Innovations). Briefly, after background subtraction of the image, an automatic threshold was used to determine the percentage of positive surface area (i.e. pixels above threshold) belonging to the hand-drawn mandibular area. Average and *t*-test statistics were calculated using Excel (Microsoft).

Acknowledgements

We thank R. Erzurumlu and G. Levi for discussions at an early stage of the project. We also wish to thank F. Wang for the kind gift of probes and S. Ducret for excellent technical assistance.

Competing interests

The authors declare no competing or financial interests.

Author contributions

C.L. performed most of the experimental work, quantifications, and documentation. A.B. carried out several tracing experiments, identified the *Cdh13* marker, some quantification experiments, and additional unpublished results relevant for the study. N.V. carried out several single and double *in situ* hybridisations, and relative documentation. C.L., A.B., N.V. and F.M.R. designed and analysed the experiments. Y.K. and H.K. provided extensive access to and production of essential biological samples, discussions throughout the work, and comments on draft. F.M.R. conceived the study, and C.L. and F.M.R. wrote the manuscript.

Funding

A.B. was supported by a European Molecular Biology Organization long-term postdoctoral fellowship. Work in F.M.R. laboratory is supported by the Swiss National Science Foundation [31003A_149573], L'Association pour l'aide à la recherche sur la sclérose en plaques (ARSEP), and the Novartis Research Foundation.

Supplementary information

Supplementary information available online at
http://dev.biologists.org/lookup/suppl/doi:10.1242/dev.128736/-/DC1

References

Arvidsson, J. and Rice, F. L. (1991). Central projections of primary sensory neurons innervating different parts of the vibrissae follicles and intervibrissal skin on the mystacial pad of the rat. *J. Comp. Neurol.* **309**, 1-16.

Clouthier, D. E., Hosoda, K., Richardson, J. A., Williams, S. C., Yanagisawa, H., Kuwaki, T., Kumada, M., Hammer, R. E. and Yanagisawa, M. (1998). Cranial and cardiac neural crest defects in endothelin-A receptor-deficient mice. *Development* **125**, 813-824.

Cohen-Tannoudji, M., Babinet, C. and Wassef, M. (1994). Early determination of a mouse somatosensory cortex marker. *Nature* **368**, 460-463.

da Silva, S., Hasegawa, H., Scott, A., Zhou, X., Wagner, A. K., Han, B.-X. and Wang, F. (2011). Proper formation of whisker barrelettes requires periphery-derived Smad4-dependent TGF-beta signaling. *Proc. Natl. Acad. Sci. USA* **108**, 3395-3400.

Erzurumlu, R. S. and Jhaveri, S. (1992). Trigeminal ganglion cell processes are spatially ordered prior to the differentiation of the vibrissa pad. *J. Neurosci.* **12**, 3946-3955.

Erzurumlu, R. S. and Killackey, H. P. (1983). Development of order in the rat trigeminal system. *J. Comp. Neurol.* **213**, 365-380.

Erzurumlu, R. S., Chen, Z.-F. and Jacquin, M. F. (2006). Molecular determinants of the face map development in the trigeminal brainstem. *Anat. Rec. A Discov. Mol. Cell. Evol. Biol.* **288A**, 121-134.

Erzurumlu, R. S., Murakami, Y. and Rijli, F. M. (2010). Mapping the face in the somatosensory brainstem. *Nat. Rev. Neurosci.* **11**, 252-263.

Grove, E. A. and Fukuchi-Shimogori, T. (2003). Generating the cerebral cortical area map. *Annu. Rev. Neurosci.* **26**, 355-380.

Hodge, L. K., Klassen, M. P., Han, B.-X., Yiu, G., Hurrell, J., Howell, A., Rousseau, G., Lemaigre, F., Tessier-Lavigne, M. and Wang, F. (2007). Retrograde BMP signaling regulates trigeminal sensory neuron identities and the formation of precise face maps. *Neuron* **55**, 572-586.

Jensen-Smith, H., Gray, B., Muirhead, K., Ohlsson-Wilhelm, B. and Fritzsch, B. (2007). Long-distance three-color neuronal tracing in fixed tissue using NeuroVue dyes. *Immunol. Invest.* **36**, 763-789.

Kurihara, Y., Kurihara, H., Suzuki, H., Kodama, T., Maemura, K., Nagai, R., Oda, H., Kuwaki, T., Cao, W.-H., Kamada, N. et al. (1994). Elevated blood pressure and craniofacial abnormalities in mice deficient in endothelin-1. *Nature* **368**, 703-710.

Lee, L.-J., Lo, F.-S. and Erzurumlu, R. S. (2005). NMDA receptor-dependent regulation of axonal and dendritic branching. *J. Neurosci.* **25**, 2304-2311.

Lokmane, L., Proville, R., Narboux-Nême, N., Györy, I., Keita, M., Mailhes, C., Léna, C., Gaspar, P., Grosschedl, R. and Garel, S. (2013). Sensory map transfer to the neocortex relies on pretarget ordering of thalamic axons. *Curr. Biol.* **23**, 810-816.

López-Bendito, G. and Molnár, Z. (2003). Thalamocortical development: how are we going to get there? *Nat. Rev. Neurosci.* **4**, 276-289.

Ma, P. M. (1991). The barrelettes - architectonic vibrissal representations in the brainstem trigeminal complex of the mouse. I. Normal structural organization. *J. Comp. Neurol.* **309**, 161-199.

Development (2015) 142, 3704-3712 doi:10.1242/dev.128736

Ma, P. M. (1993). Barrelettes - architectonic vibrissal representations in the brainstem trigeminal complex of the mouse. II. Normal post-natal development. *J. Comp. Neurol.* **327**, 376-397.
Ma, P. M. and Woolsey, T. A. (1984). Cytoarchitectonic correlates of the vibrissae in the medullary trigeminal complex of the mouse. *Brain Res.* **306**, 374-379.
Ohsaki, K., Osumi, N. and Nakamura, S. (2002). Altered whisker patterns induced by ectopic expression of Shh are topographically represented by barrels. *Dev. Brain Res.* **137**, 159-170.
O'Leary, D. D. M., Chou, S.-J. and Sahara, S. (2007). Area patterning of the mammalian cortex. *Neuron* **56**, 252-269.
Oury, F., Murakami, Y., Renaud, J.-S., Pasqualetti, M., Charnay, P., Ren, S.-Y. and Rijli, F. M. (2006). Hoxa2- and rhombomere-dependent development of the mouse facial somatosensory map. *Science* **313**, 1408-1413.
Ozdinler, P. H. and Erzurumlu, R. S. (2002). Slit2, a branching-arborization factor for sensory axons in the Mammalian CNS. *J. Neurosci.* **22**, 4540-4549.
Ozeki, H., Kurihara, Y., Tonami, K., Watatani, S. and Kurihara, H. (2004). Endothelin-1 regulates the dorsoventral branchial arch patterning in mice. *Mech. Dev.* **121**, 387-395.
Schlaggar, B. L. and O'Leary, D. D. (1993). Patterning of the barrel field in somatosensory cortex with implications for the specification of neocortical areas. *Perspect. Dev. Neurobiol.* **1**, 81-91.
Stirling, R. V., Liestøl, K., Summerbell, D. and Glover, J. C. (1995). The segmental precision of the motor projection to the intercostal muscles in the developing chicken embryo: a differential labelling study using fluorescent tracers. *Anat. Embryol.* **191**, 397-406.
Sur, M. and Rubenstein, J. L. R. (2005). Patterning and plasticity of the cerebral cortex. *Science* **310**, 805-810.
Van Der Loos, H. (1976). Barreloids in mouse somatosensory thalamus. *Neurosci. Lett.* **2**, 1-6.
Van der Loos, H., Dorfl, J. and Welker, E. (1984). Variation in pattern of mystacial vibrissae in mice. A quantitative study of ICR stock and several inbred strains. *J. Hered.* **75**, 326-336.
Wong-Riley, M. (1979). Columnar cortico-cortical interconnections within the visual system of the squirrel and macaque monkeys. *Brain Res.* **162**, 201-217.
Woolsey, T. A. and Van der Loos, H. (1970). The structural organization of layer IV in the somatosensory region (SI) of mouse cerebral cortex: the description of a cortical field composed of discrete cytoarchitectonic units. *Brain Res.* **17**, 205-242.
Xiang, C., Zhang, K.-H., Yin, J., Arends, J. J. A., Erzurumlu, R. S., Jacquin, M. F. and Chen, Z.-F. (2010). The transcription factor, Lmx1b, is necessary for the development of the principal trigeminal nucleus-based lemniscal pathway. *Mol. Cell. Neurosci.* **44**, 394-403.

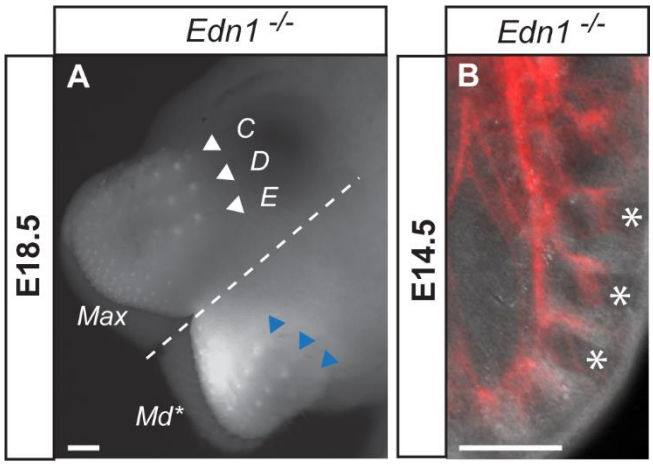

Supplementary Figure S1. Morphology and innervation of ectopic whisker pad in Edn1-/- embryo

(A) Face of Edn1-/- mouse at E18.5 showing homeotic transformation of distal mandibular process into maxillary-like structure, including the partial duplication of the whisker pad and three ectopic rows (blue arrows). **(B)** Transverse section through the ectopic whisker pad of Edn1-/- embryo at E14.5, which mandibular branch of the trigeminal nerve was labelled with NeuroVue®, showing innervation (red) around the ectopic whisker follicles (asterisks). Scale bar 100 and 50µm in **A** and **B** respectively.

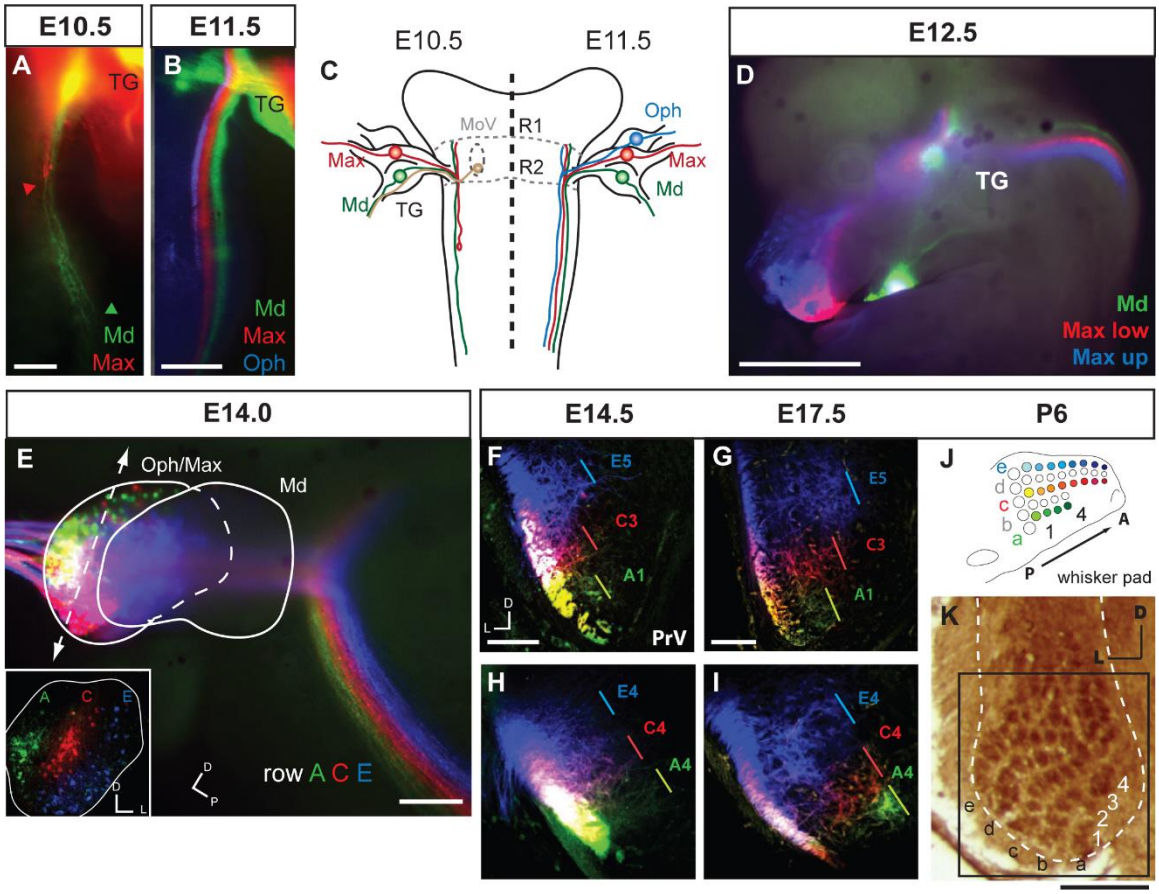

Supplementary Figure S2. Topographic segregation of facial sensory inputs during development

(A-B) Ventral view of a flatted neural tube after labelling of the face in mandibular (Md-*green*) and maxillary (Max-*red*) presumptive domain at E10.5 **(A)** and labelling of the mandibular process (Md-*green*), and in lower (Max-*red*) and upper (Oph-*blue*) positions of the upper jaw at E11.5 **(B)**. Central projections of trigeminal mandibular neurons are the first to reach posterior hindbrain at E10.5 quickly followed by the rest of trigeminal neurons projections at E11.5 showing a differential timing of elongation, summarized in **(C)**. **(D)** Whole mount view of E12.5 embryo after labelling in mandibular (Md-*green*), lower (Max low-*red*) and upper (Max up-*blue*) whisker pad areas showing maintenance of sensory inputs segregation from the periphery to the brain. **(E)** Sagittal view of E14 embryo after labelling of rows A, C and E in the whisker pad showing a

ventro-dorsal segregation of maxillary inputs within the brainstem somatosensory tract and also latero-medial segregation of trigeminal neurons within TG (inset). **(F-K)** Coronal sections of the hindbrain at PrV level after labelling in positions A1-C3-E5 (green-red-blue) **(F, G)** and positions A4-C4-E4 (green-red-blue) **(H, I)** on the whisker pad at E14.5 **(F, H)** and E17.5 **(G, I)** respectively. Collaterals sent by sensory axons reach different latero-medial positions in the nucleus according to their peripheral antero-posterior location within a row **(J)**. This collateralization process take place in respect of the whisker position in the mature map of the PrV nucleus revealed at P6 with cytochrome oxidase staining **(K)**. Scale bar: **A** is 25µm, **B** is 50µm, **D** is 200µm, **E**, **F**, **G** and **K** are 100µm. **F** and **G** represents **F** and **H** and **G** and **I** respectively.

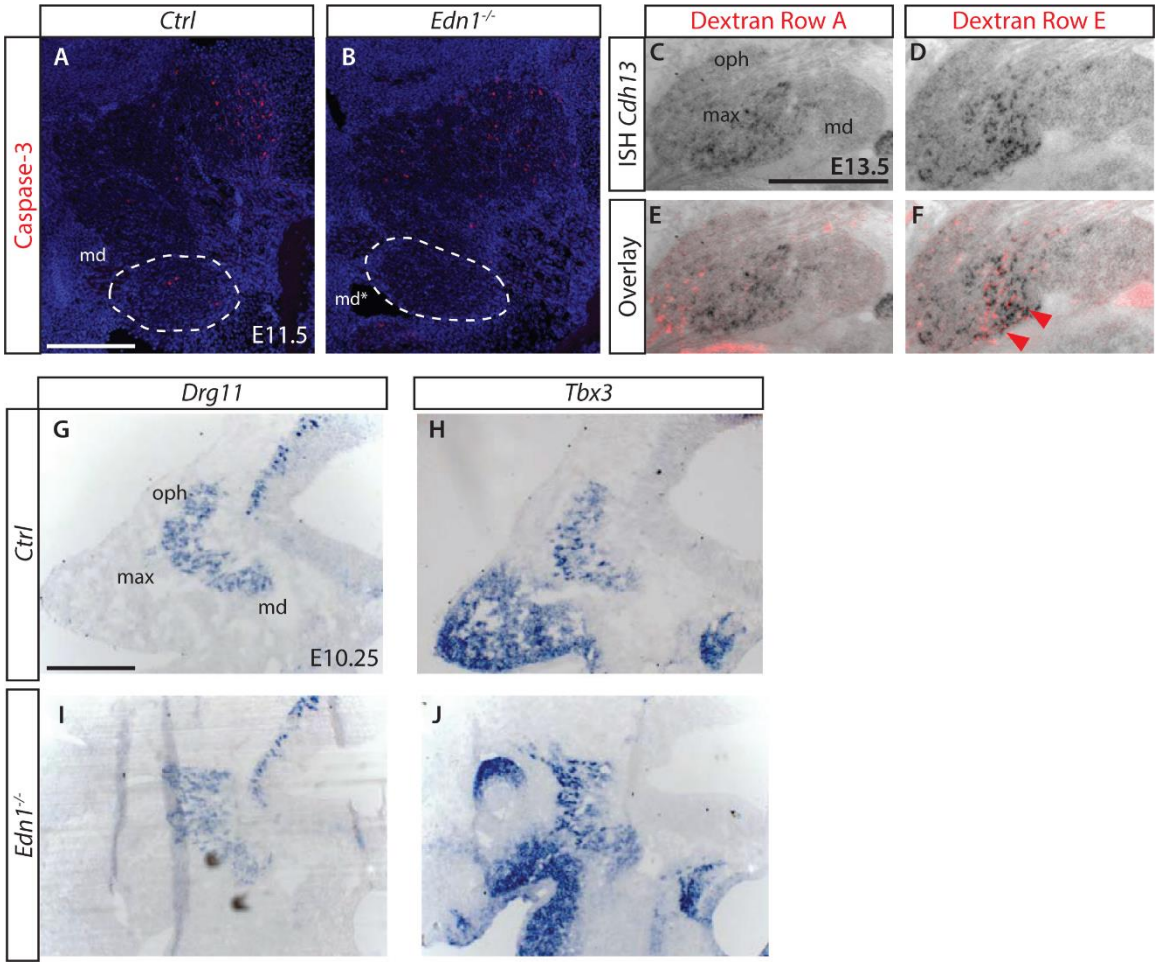

Supplementary Figure S3. Supporting information for molecular changes observed in TG of Edn1$^{-/-}$ embryos

(A-B) Immunochemistry against Caspase-3 of sagittal sections through TG of control (*Ctrl*) **(A)** and *Edn1-/-* embryos **(B)**. No increase in staining was observed at E11.5 in the mandibular portion of the TG (dash line) in *Edn1*$^{-/-}$ following innervation of ectopic array of whiskers. (**C-F**) in situ hybridisation for Cdh13 on sagittal section through TG of *Ctrl* embryos at E13.5 previously labelled with Biotin-conjugated Dextran in row A (**C,E**) and E (**D,F**). Overlay of in situ and Dextran show that *Cdh13* expression mostly collocalize with TG cell bodies retrogradely labelled from row E (**F**) compare to row A (**E**). (**G-L**) in situ hybridisation on sagittal section through TG of *Ctrl* (**G-I**) and *Edn1*$^{-/-}$ (**J-L**) embryos at E10.25. *Drg11*, *Tbx3* and *OC1* do not display noticeable difference of expression between *Ctrl* and *Edn1*$^{-/-}$ embryos. Scale bar: A is 50µm, C is 100µm and G is 25µm and applies for **A-B**, **C-F** and **G-L** respectively.

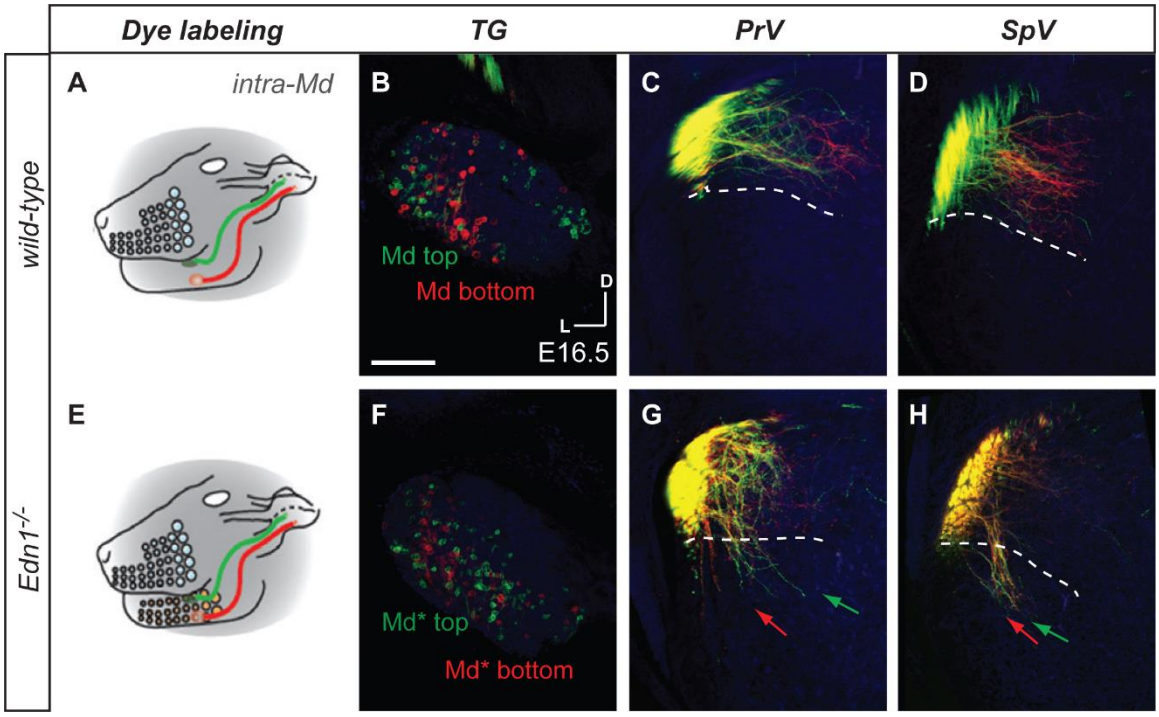

Supplementary Figure S4. Lack of segregation of mandibular central axon projections after redirection from dorsal to ventral PrV and SpV in *Edn1*$^{-/-}$ foetuses

(A-H) Labelling of distinct positions of the maxillary and mandibular process at E16.5 in wild type **(B-D)** and *Edn1*$^{-/-}$ **(F-H)** embryos. **(A,E)** Schematic depiction of peripheral dye labelling of upper(*green*) and lower(*red*) mandibular positions corresponding to sections (**B-D,F-H**). Coronal sections through TG **(B,F)**, PrV **(C,G)** and SpV **(D,H)**. Ectopic whisker-innervating Md* collaterals turn from dPrV and dorsal SpV, and navigate into vPrV and ventral SpV (arrows, **G,H**). Labelling of two distinct dorso-ventral positions on the ectopic whisker pad shows that Md* neuron cell bodies (**F**) do not acquire a segregated organisation but remain intermingled as wild type Md neuron cell bodies (**B**). No clear sorting of collaterals navigating into vPrV or ventral SpV is observed (red and green arrows, **G,H**). Scale bar in **B** is 50 µm and represents **B-D**, **F-H**.